(Received 10 November 2024, Accepted 26 December 2024, Scheduled 27 December 2024)

Three-Dimensional Topological Photonic Crystals

Jian-Wei Liu[1,*], Gui-Geng Liu[2,3,*], and Baile Zhang[1,4,*]

[1] *Division of Physics and Applied Physics, School of Physical and Mathematical Sciences Nanyang Technological University, Singapore 637371, Singapore*
[2] *Research Center for Industries of the Future, Westlake University, Hangzhou 310030, China*
[3] *Department of Electronic and Information Engineering, School of Engineering, Westlake University, Hangzhou 310030, China*
[4] *Centre for Disruptive Photonic Technologies, The Photonics Institute Nanyang Technological University, Singapore 637371, Singapore*

ABSTRACT: Photonic crystals, often referred to as the "semiconductors of light," have entered a new phase enabling exotic properties once exclusive to topological quantum matter such as topological insulators. While the development of the first three-dimensional (3D) photonic crystal marked the establishment of photonic crystals as an independent field, initial studies in topological photonic crystals focused mainly on one and two dimensions. Though a true photonic crystal counterpart of a 3D strong topological insulator remains elusive, significant progress has been made toward achieving 3D topological photonic crystals. Compared with their lower-dimensional counterparts, 3D topological photonic crystals reveal a richer variety of topological phases and surface manifestation, which enables more degrees of freedom for light manipulation. In this review, concentrating on the novel boundary states unique in 3D systems, we provide a brief survey of the 3D topological photonic crystals and recent advances in this field. We categorize and discuss various topological phases and associated phenomena observed in 3D photonic crystals, including both gapped and gapless phases. Additionally, we delve into some recent developments in this rapidly evolving area, including the realization of 3D topological phases through synthetic dimensions.

1. INTRODUCTION

Almost four decades ago, Yablonovitch [1] and John [2] proposed the concept of photonic crystals, commonly referred to as the "semiconductors of light". Their first pursuit was a three-dimensional (3D) structure that exhibits a full photonic bandgap — as inspired from semiconductor's bandgap — in which electromagnetic wave propagation is forbidden in all directions [3–8]. While the history of one-dimensional (1D) photonic bandgap (e.g., in a Bragg mirror) can be traced back to Rayleigh's time in 1887, it is this 3D photonic crystal that marked the establishment of photonic crystals as an impactful independent field in photonics. Since then, many 3D photonic crystals have been realized with plenty of applications such as laser cavities and photonic integrated circuits, typically involving a few degrees of freedom (DOFs), such as frequency, polarization, and phase [9–14].

The main motivation in the emerging field of topological photonics is to introduce topology as a new DOF into the design and construction of photonic systems, typically in photonic crystals [15–18]. A common practice in topological photonics is to map Maxwell's equations into the electronic Schrodinger equation. While there exits distinction between light (vector wave) and electronic wavefunction (scalar wave), this mapping works well in 2D [19–32], because the two polarizations of light can be decoupled and each polarization can be treated as a scalar wave. For example, in the first so-called "photonic topological insulator", a photonic crystal was demonstrated to exhibit non-trivial Chern number and chiral edge states [20, 21], similar to the quantum Hall effect. Therefore, the relatively intuitive design and simpler fabrication demand makes 2D topological photonic systems hold great promise with exciting applications such as topological photonic circuits [33–35]. In addition, the inadequate light confinement induces radiative coupling in 2D systems, which leads to research fields such as topological lasers [36–38] and metasurface [39, 40].

Compared with 2D, light is intrinsically vectorial and volumetric in 3D, making the construction of 3D topological phases in photonics fundamentally more difficult in both theory and experiment. Nevertheless, the topologically protected omnidirectional photonic band gap makes 3D topological photonic crystals a potential platform for achieving ultra-strong light localization and consequently enhanced light-matter interaction. This potential mirrors the historical trajectory of conventional 3D photonic crystals, which is born to be recognized in light-matter interaction due to the omnidirectional photonic band gap. Additionally, the extra spatial DOF in 3D systems provides more tunable parameters, leading to a richer variety of topological phases, which are broadly classified into gapped and gapless categories. The 3D gapped topological phases can be seen as extensions of the 2D "Hall family", while the 3D gapless topological semimetals, exhibiting point or line degeneracies where two bands intersect in the 3D Brillouin zone (BZ), have no 2D counterpart [41–43]. More importantly, the additional spatial dimension in 3D systems further enables versatile control over light, including 2D surface states (Figs. 1(a) and 1(b)), 1D light propagation channels (hinge states in Fig. 1(c)),

* Corresponding authors: Jian-Wei Liu (jianwei.liu@ntu.edu.sg); Gui-Geng Liu (liuguigeng@westlake.edu.cn); Baile Zhang (blzhang@ntu.edu.sg).

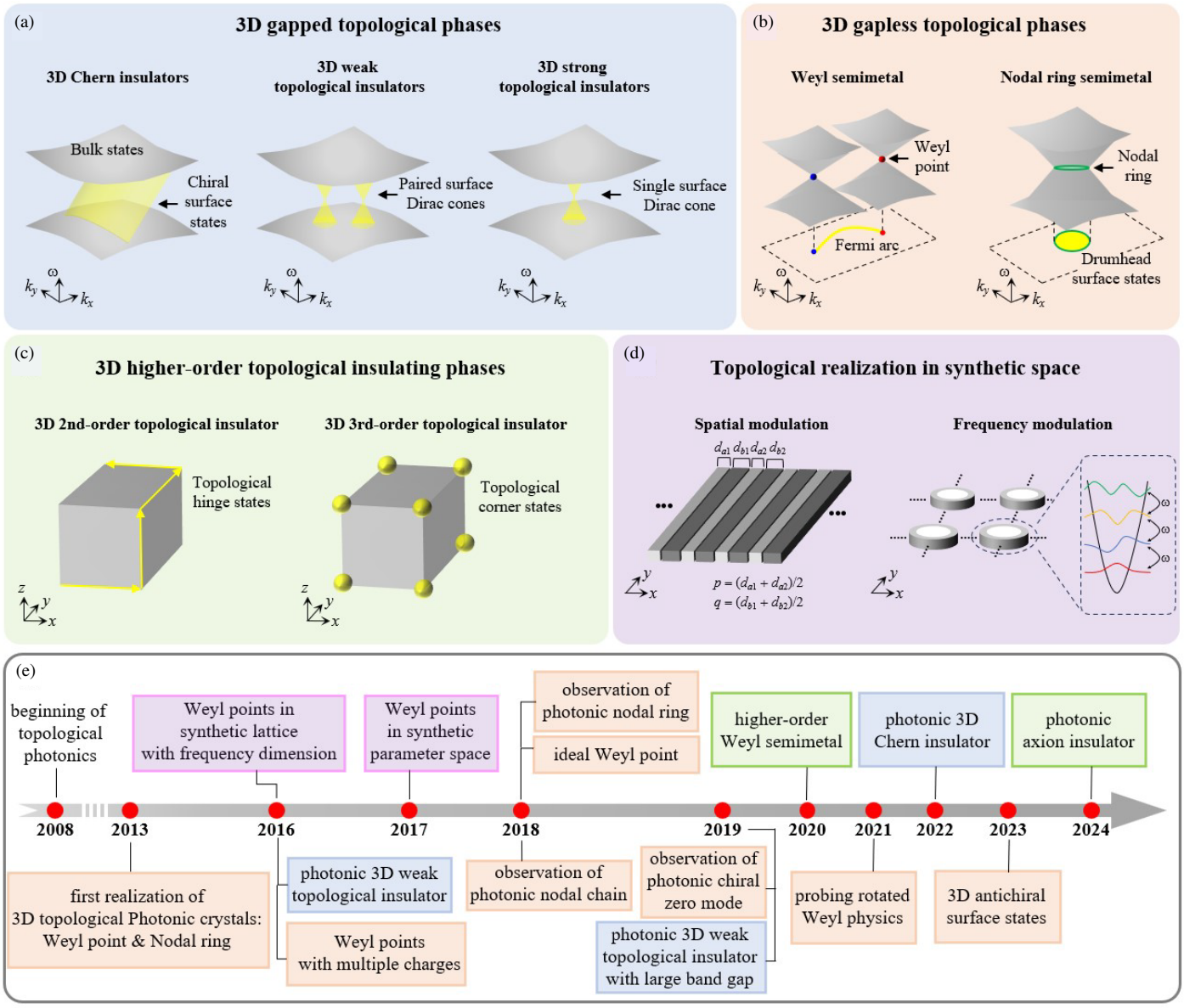

FIGURE 1. Schematic illustration of different 3D photonic topological phases and the roadmap of 3D topological photonic crystals. (a) Dispersion and corresponding surface states of 3D gapped topological phases. (b) Dispersion and corresponding surface states of 3D gapless topological phases. (c) Manifestations of 3D higher-order topological phases. (d) Different approaches to realize topological phases in synthetic space. (e) Evolutionary roadmap of 3D topological photonic crystals.

and 0D localized modes (corner states in Fig. 1(c)). For example, a 2D chiral surface state could be supported at the surface of photonic 3D Chern insulator (left panel in Fig. 1(a)) [44], while a pair of surface Dirac cones exist at the surface of weak topological insulator (middle panel of Fig. 1(a)) [45, 46]. Similarly, as shown in Fig. 1(b), the Fermi arc can exist at the boundary of the photonic Weyl semimetal, connecting two Weyl points with opposite chirality [47, 48].

Although the fundamental differences make it challenging to transfer condensed-matter concepts directly to topological photonics in 3D, some breakthroughs have been achieved. The first realization of photonic 3D topological phases was demonstrated in double-gyroid photonic crystals, revealing the existence of Weyl points and nodal rings in photonic systems [49]. Furthermore, photonic 3D weak topological insulators have been achieved in time-reversal invariant systems, by vertically stacking photonic 2D quantum spin Hall insulators [45, 46]. Most recently, the photonic 3D Chern insulators have been realized in 3D gyromagnetic photonic crystals [44], complementing the family of 3D magnetic topological phases. However, unlike the early history of photonic crystals that began with a 3D photonic crystal, so far, a 3D photonic crystal exhibiting properties of a 3D strong topological insulator remain elusive. Fig. 1(e) shows a roadmap of 3D topological photonic crystals, which provides a relatively clearer development of this field.

Here, concentrating on the novel boundary states unique in 3D systems, we review the latest developments in 3D topological photonic crystals. We will classify and discuss various topo-

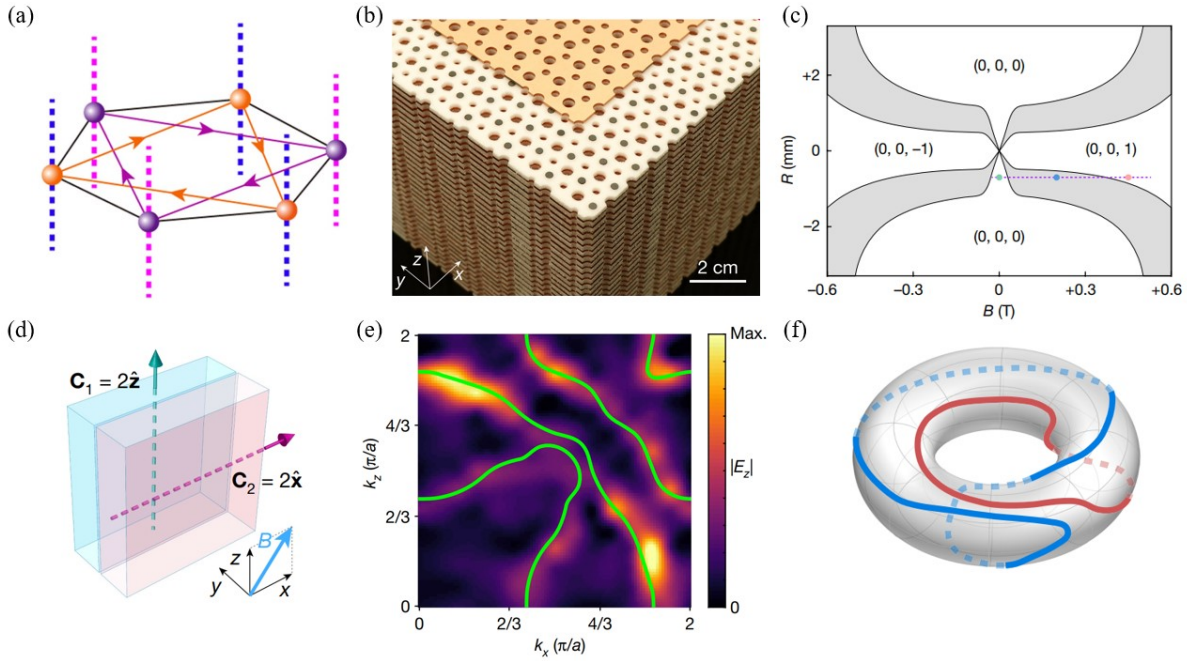

FIGURE 2. Photonic 3D Chern insulators. (a) 3D Haldane model. (b) Photograph of the photonic 3D Chern insulator. The unit cell of this structure is comprised of a YIG rod placed atop a metallic plate. (c) Phase diagram of the photonic 3D Chern insulator. The gray regions represent the intermediate Weyl phase. (d) Illustration of an interface between two photonic 3D Chern insulators with perpendicular Chern vectors $\mathbf{C}_1 = (0, 0, 2)$ and $\mathbf{C}_2 = (2, 0, 0)$. (e) Surface intensity on the interface BZ. Green lines indicate Fermi loop surface states. (f) Fermi loops wrap around the surface BZ torus to form a Hopf-link.
All figures reproduced from Ref. [44], Copyright 2022, Springer Nature.

logical phases and associated phenomena observed in 3D photonic crystals, including both gapped and gapless phases. In addition, we will delve into some recent developments, including the realization of 3D topological phases through synthetic dimensions (Fig. 1(d)) and the realization of higher-order topological phases in 3D photonic crystals (Fig. 1(c)).

2. GAPPED PHASES IN 3D TOPOLOGICAL PHOTONIC CRYSTALS

As the research focus of 2D topological photonics lies in the gapped bulk bands and the associated topological edge states, a logically straightforward strategy to construct photonic 3D topological phases is to extend the 2D topological phases into 3D systems. Similar to the 2D counterparts, the 3D gapped phases include 3D Chern insulators [44, 50, 51] (described by the Chern vector) and 3D topological insulators [45, 46, 52–55] (described by Z_2 index).

2.1. Photonic 3D Chern Insulators

While the photonic 2D Chern insulator was historically inspired by the 2D Haldane model, a photonic 3D Chern insulator can be designed by following a 3D Haldane model. As depicted in Fig. 2(a), a 3D Haldane model can be constructed by layering the 2D one [56]. Within each layer, the model is identical to the original 2D Haldane model, while between layers are interlayer hopping terms for A and B sublattice. In photonics, such model was realized by using the 3D gyromagnetic photonic crystals [44], as shown in Fig. 2(b). The unit cell of this structure is comprised of a gyromagnetic Yttrium-Iron-Garnet (YIG) rod placed atop a metallic plate. The YIG rods, subjected to an external magnetic field, break time-reversal symmetry (T), while small coupling holes with different radii in the metallic plates break the inversion symmetry (P). By modulating the magnetic field strength and the size of the coupling holes, the photonic crystal exhibits a phase diagram (Fig. 2(c)) that includes trivial insulators, 3D Chern insulators, and intermediate Weyl phases [grey regions; the Weyl semimetal phase will be discussed in the following section]. Since the Chern number is ill-defined in 3D spaces, the 3D Chern insulator can be characterized by a Chern vector consisting of three Chern numbers $\mathbf{C} = (C_x, C_y, C_z)$, with each Chern number defined for a 2D sliced BZ oriented in one of the three orthogonal directions [57, 58], similar to the 3D quantum Hall effect.

Distinct from the scalar Chern number in 2D systems, the vectorial Chern vector can render richer topological manifestation. For instance, a non-trivial Chern vector gives rise to the 2D chiral surface states. Like the unidirectional 1D chiral edge states in the photonic 2D Chern insulators, the chiral surface state circulates anticlockwise around the photonic 3D Chern insulator, and can navigate around sharp bends and large obstacles without backscattering. In momentum space, the chiral surface states winding around the surface BZ, forming the surface Fermi loops. Moreover, by considering an interface between two 3D photonic Chern insulators with perpendicular Chern vectors (Fig. 2(d)), the vectorial nature of the Chern vector can be further validated. As shown in Fig. 2(e), the Fermi

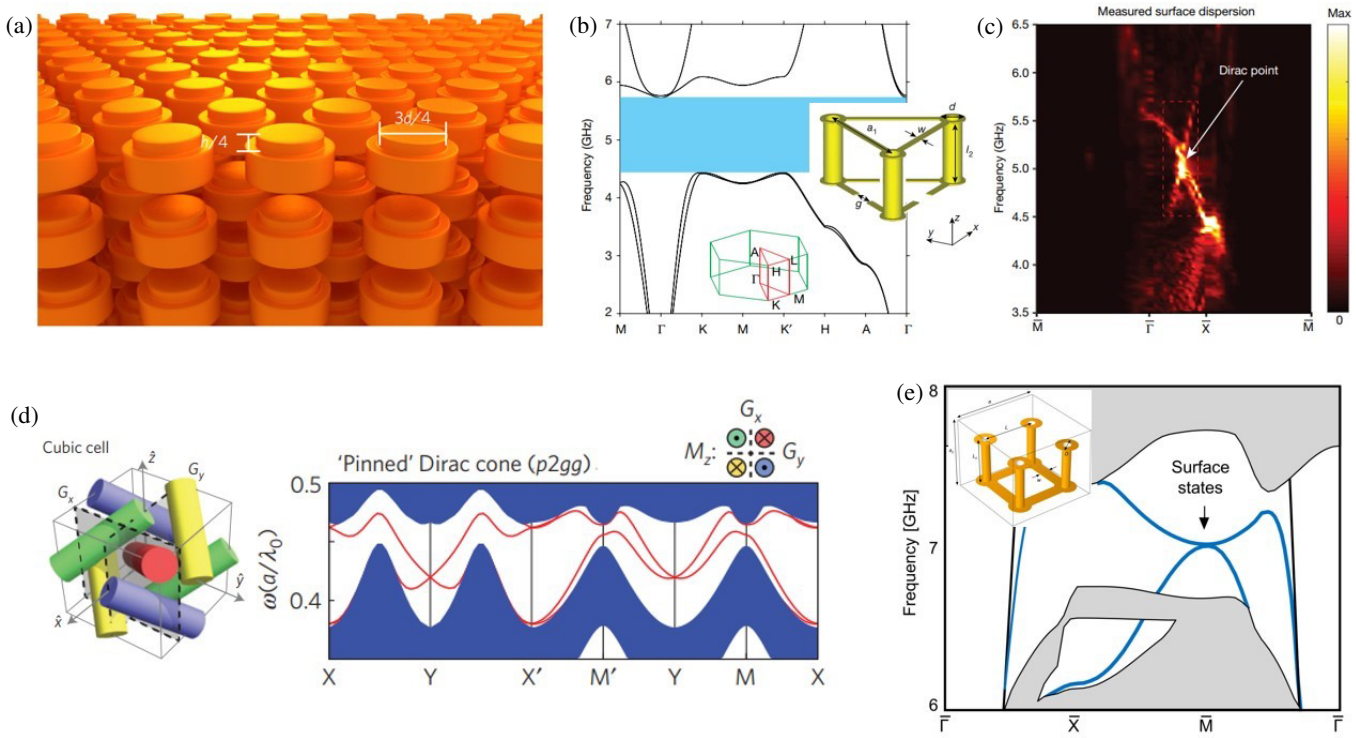

FIGURE 3. Photonic 3D topological insulators. (a) Bianisotropic induced photonic 3D weak topological insulators. (b) Photonic 3D weak topological insulators with extremely large bandgap. (c) Measured gapless Dirac-cone-like surface states in split-ring resonators. (d) Photonic 3D topological crystalline insulator in a 3D gyroelectric photonic crystal. (e) Time-reversal-invariant photonic 3D topological crystalline insulators with quadratic surface dispersion.
Figures reproduced from: (a) Ref. [45], Copyright 2017, Springer Nature; (b), (c) Ref. [46], Copyright 2019, Springer Nature; (d) Ref. [52], Copyright 2016, Springer Nature; (e) Ref. [54], Copyright 2022, Springer Nature.

loops caused by the two domains winding simultaneously in the surface BZ. Because of the avoid-crossing principle, theses Fermi loops can form topological links or knots in the surface torus (e.g., a Hopf link shown in Fig. 2(f)), according to the knot theory.

2.2. Photonic 3D Topological Insulators

Distinct from the chiral surface states in photonic 3D Chern insulators, the Dirac-cone-like surface state, known as the surface Dirac cone, is a significant manifestation in photonic 3D topological insulators. Characterized by the topological invariant of Z_2 index, the photonic 3D topological insulators can be classified into weak and strong types [59]. However, besides the Z_2 index, a rule of thumb to tell one type from another is the number of the surface Dirac cones: the photonic 3D weak topological insulators have an even number of surface Dirac cones, while the strong ones possess an odd number.

The electromagnetic duality and bianisotropy have been used to realize the topological quantum spin Hall phase in 2D topological photonic crystals. It has been known that the stacking of the 2D topological insulators with proper interlayer couplings can give rise to a 3D weak topological insulator. Following this approach, a photonic 3D weak topological insulator with an even number of surface Dirac cones was theoretically proposed (structure shown in Fig. 3(a)) [45]. However, despite the elegance of the above proposal based on dielectric materials, the 3D topological bandgap has a narrow fractional bandwidth of only about 1%, making the experimental realization challenging. Subsequently, a photonic 3D topological insulator with a broad topological bandgap was proposed by using a 3D array of metallic split-ring resonators [46]. Due to the strong bianisotropy, this photonic 3D topological insulator possesses an extremely large 3D topological bandgap with a fractional bandwidth up to 25%, which significantly exceeds the previously proposed 3D photonic topological bandgaps, as depicted in Fig. 3(b). The wide 3D bandgap further facilitates the experimental demonstration. Indeed, a fully gapped bulk dispersion and a pair of surface Dirac cones in the 3D bandgap were directly visualized at the boundary (Fig. 3(c)).

Unlike photonic 3D weak topological insulators, photonic 3D strong topological insulators have an odd number of surface Dirac cones. A typical design can be achieved using magnetically biased gyroelectric materials, as shown in Fig. 3(d) [52]. Nevertheless, due to the experimental challenges in implementation of complex magnetization, this photonic 3D strong topological insulator has not been realized thus far. While most 3D strong topological insulators protected by the fermionic T, this photonic 3D strong topological insulator is protected by the nonsymmorphic glide reflection of the underlying lattice. Thus,

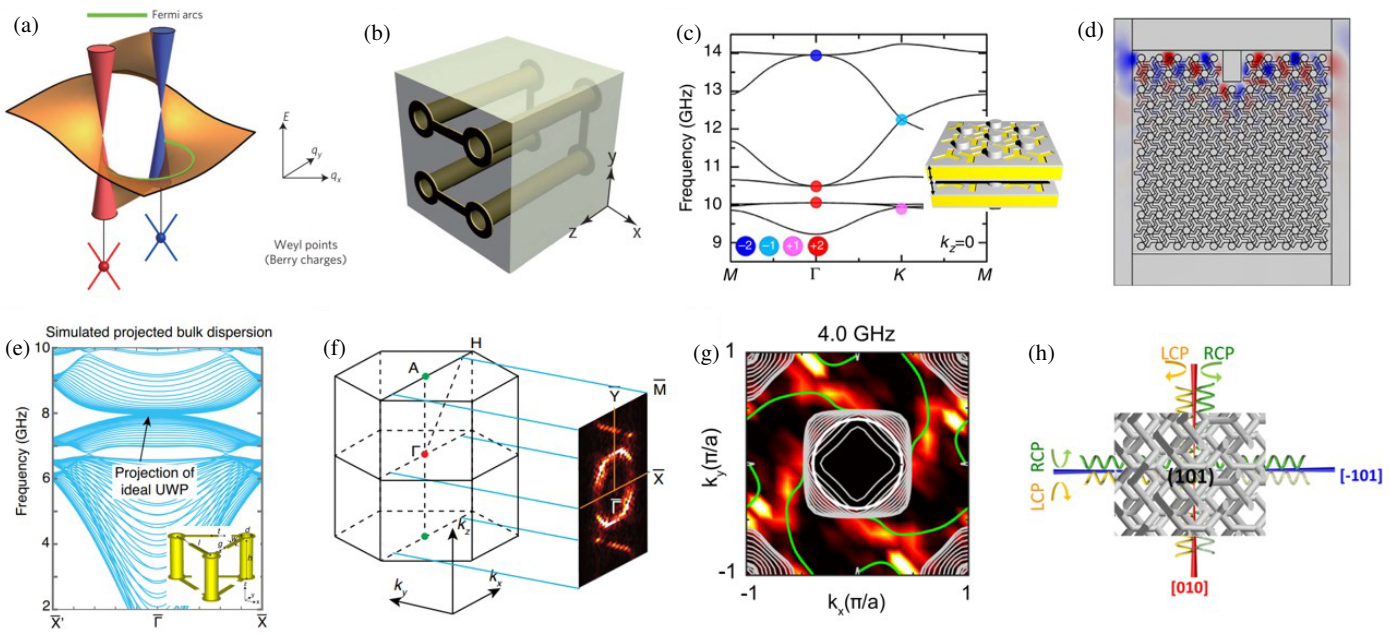

FIGURE 4. 3D photonic crystals possessing Weyl semimetal phase. (a) Schematic of the helicoidal Riemann surface states and Fermi arc. (b) Ideal Weyl points in 3D photonic crystal of saddle-shaped metallic coils. (c) Multiple Weyl points in stacked metallic photonic crystals. (d) Robust surface states between the Weyl photonic crystal and the perfect electric conductor. (e) Ideal charge-2 Weyl points in chiral metallic photonic crystals. (f) Noncontractible loops wrapping around the surface BZ. (g) Quadruple-helicoid Fermi arcs in the maximally charged photonic Weyl semimetal. (h) The chirality of the Weyl points results in the coupling of spin-angular momentum of light.
Figures reproduced from: (a) Ref. [86], Copyright 2016, Springer Nature; (b) Ref. [47], Copyright 2018, The American Association for the Advancement of Science; (c), (d) Ref. [48], Copyright 2016, Springer Nature; (e), (f) Ref. [66], Copyright 2020, American Physical Society; (g) Ref. [68], Copyright 2022, Springer Nature; (h) Ref. [70], Copyright 2017, Wiley-VCH.

it can also be regarded as a 3D topological crystalline insulator. Actually, the photonic 3D topological crystalline insulators with preserved bosonic T can also exist. As shown in Fig. 3(e), a T-invariant photonic 3D topological crystalline insulator can be realized with split-ring resonators [54]. Different from the Dirac-cone-like surface states in photonic 3D weak topological insulators, the surface states of this photonic 3D topological crystalline insulators possess a quadratic dispersion.

3. GAPLESS PHASES IN 3D TOPOLOGICAL PHOTONIC CRYSTALS

The discovery of topological gapless phases, also known as topological semimetal phase, has broadened our understanding, challenging the notion that non-trivial band topology can only exist in gapped systems. Instead of non-trivial band gaps, the defining feature of topological semimetal phases is the presence of band degeneracies, where two or more bands intersect at specific momentum points in the 3D BZ. These band degeneracies can be categorized based on their dimensionality, including 0D nodal points (Weyl points [47–49, 60–70]/Dirac points [71–74]), 1D nodal lines [75–83], and 2D nodal surfaces [84, 85].

3.1. Weyl Point

Weyl point is a prototypical example of band degeneracies in 3D topological semimetals, where two bands intersect linearly in momentum space. Governed by the Weyl Hamiltonian that incorporates all spatial DOFs, Weyl points are inherently robust against any translational-symmetry-preserved perturbations. Consequently, Weyl points can only be created or annihilated in pairs of opposite chirality — defined by the Chern number of a closed surface enclosing the Weyl point in momentum space.

As in other topological materials, Weyl semimetals support topologically protected surface states at their boundaries. Notably, as shown in Fig. 4(a), the surface states of Weyl semimetals exhibit a helicoidal Riemann surface dispersion [86]. Furthermore, at the Weyl frequency, the equifrequency contour of these surface states forms an open arc linking the Weyl points with opposite chirality, commonly referred to as the Fermi arc.

In photonics, Weyl points were first realized in a 3D photonic crystal with a double-gyroid structure [49]. However, the complicated configuration of bands around the Weyl frequency have hindered the observation of the helicoidal surface dispersion. To achieve a more straightforward Weyl system, an ideal Weyl semimetal was proposed using a microwave photonic crystal comprising saddle-shaped metallic coils (Fig. 4(b)) [47], where all Weyl points reside at the same frequency and are well-separated from other bands. Through angle-resolved microwave transmission measurements and near-field scanning technology, the Weyl structure and the associated surface Fermi arcs were experimentally observed in this system.

Beyond single Weyl points carrying a topological charge of 1, higher-charged Weyl points have also been explored and experimentally verified. Unlike single Weyl points (charge 1) with linear dispersion in all three momentum directions,

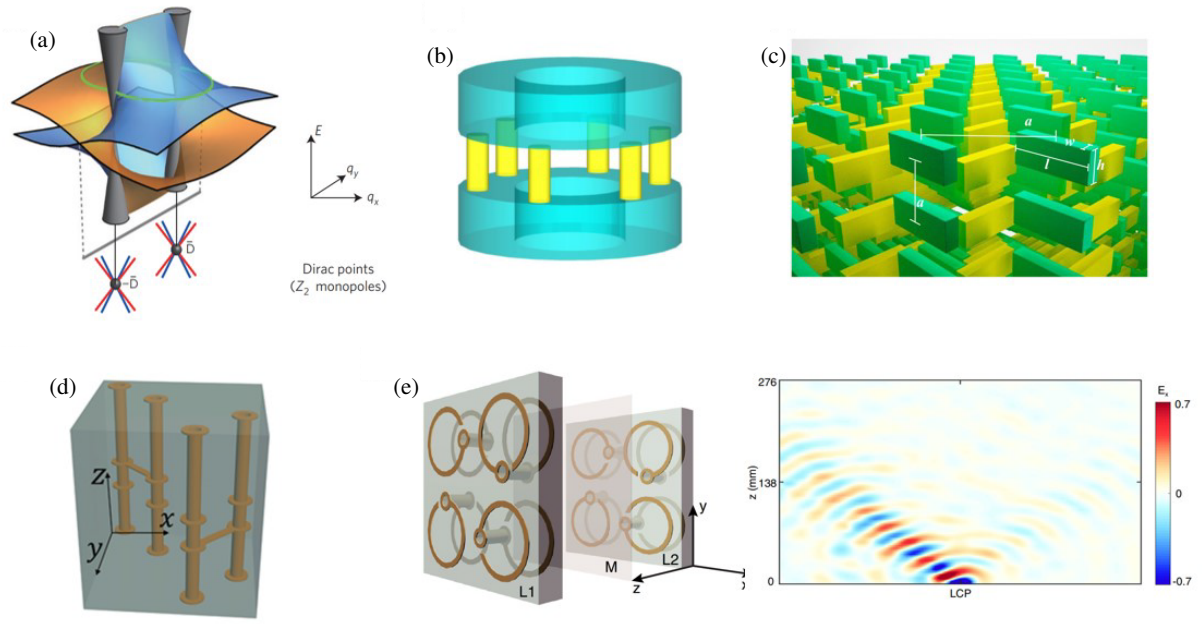

FIGURE 5. 3D photonic crystals possessing Dirac semimetal phase. (a) Schematic of the helicoidal Riemann surface states and Fermi arc in Dirac semimetals. (b) Dirac points in an all-dielectric photonic crystal, where p- and d-wave Mie resonances with double degeneracy were employed. (c) Dirac points stabilized by screw symmetry. (d) Dirac-Weyl semimetal in photonic crystals with screw symmetry but lacking inversion symmetry. (e) Experimental observation of photonic Dirac semimetals.
Figures reproduced from: (a) Ref. [86], Copyright 2016, Springer Nature; (b) Ref. [71], Copyright 2016, American Physical Society; (c) Ref. [72], Copyright 2017, Springer Nature; (d) Ref. [73], Copyright 2023, The Optica Society; (e) Ref. [74], Copyright 2019, American Physical Society.

double Weyl points (charge 2) can display quadratic dispersion. Using planar fabrication technology, photonic crystals with multiple Weyl points have been demonstrated (Fig. 4(c)) [48]. Additionally, robust surface states at the boundaries of Weyl systems were observed experimentally, for the first time (Fig. 4(d)). Multiple Weyl points present intriguing properties beyond those of single Weyl points, such as multiple topological surface states, i.e., multiple Fermi arcs. To observe these features clearly, an ideal multiple Weyl system, as shown in Fig. 4(e), is desired [66]. With the aid of microwave near-field scanning technology, the projected bulk dispersion, along with two long surface arcs forming a non-contractible loop around the surface BZ, were directly observed (Fig. 4(f)). Further investigation into multiple Weyl points revealed that the topological charge of a 2-fold Weyl point has an upper limit of 4. This maximally charged Weyl point was demonstrated in a 3D metallic photonic crystal [68]. Using microwave pump-probe spectroscopy, quadruple-helicoid Fermi arcs emanating from the charge-4 Weyl point were directly mapped out (Fig. 4(g)).

Moreover, recent advancements have led to the observation of Weyl points at optical frequencies using the galvo-dithered direct laser writing technique [70]. The coupling between circularly polarized light and Weyl points with different chirality has been demonstrated (Fig. 4(h)).

3.2. Dirac Point

Dirac points are 4-fold linearly degenerate points that occur in systems with both T and P. While Dirac points are less stable than Weyl degeneracies, they are often seen as parent or intermediate states that bridge various topological phases. For instance, when either T or P is broken, a Dirac point can split into two Weyl points with opposite chirality. Additionally, the process of gap closing and reopening at Dirac points can transition a system between topologically trivial and non-trivial phases. As the progenitor of paired Weyl points, a Dirac point also supports surface Fermi arcs at the boundaries of Dirac semimetals. However, in contrast to Weyl semimetals, two Fermi arcs emanate from a single Dirac point, as shown in Fig. 5(a).

The realization of Dirac points in photonic crystals is challenging. In electronic systems, Dirac points arise from the combination of 2-fold spin degeneracy and 2-fold orbital degeneracy. However, this is difficult to achieve in photonic crystals due to the absence of inherent spin degeneracy. Two main approaches have been explored to address this limitation. The first is to introduce additional orbital degeneracy, substituting the role of spin degeneracy. For example, by employing the p- and d-wave Mie resonances with double degeneracy, photonic Dirac semimetals were realized in an all-dielectric photonic crystal (Fig. 5(b)) [71]. The second approach involves constructing anti-unitary operators by combining T and screw rotation symmetry, mimicking the Fermionic nature. Via this approach, Dirac points can be stabilized in a photonic crystal structure with two orthogonal screw axes (Fig. 5(c)) [72]. Since Dirac points can be stabilized by screw symmetry, which relaxes the need for P, the coexistence of Weyl points and Dirac points becomes possible. In a metallic photonic crystal with screw symmetry but lacking P, the photonic Dirac-Weyl semimetal phase was demonstrated (Fig. 5(d)) [73]. In this system, Dirac points are protected at the hinges of the BZ

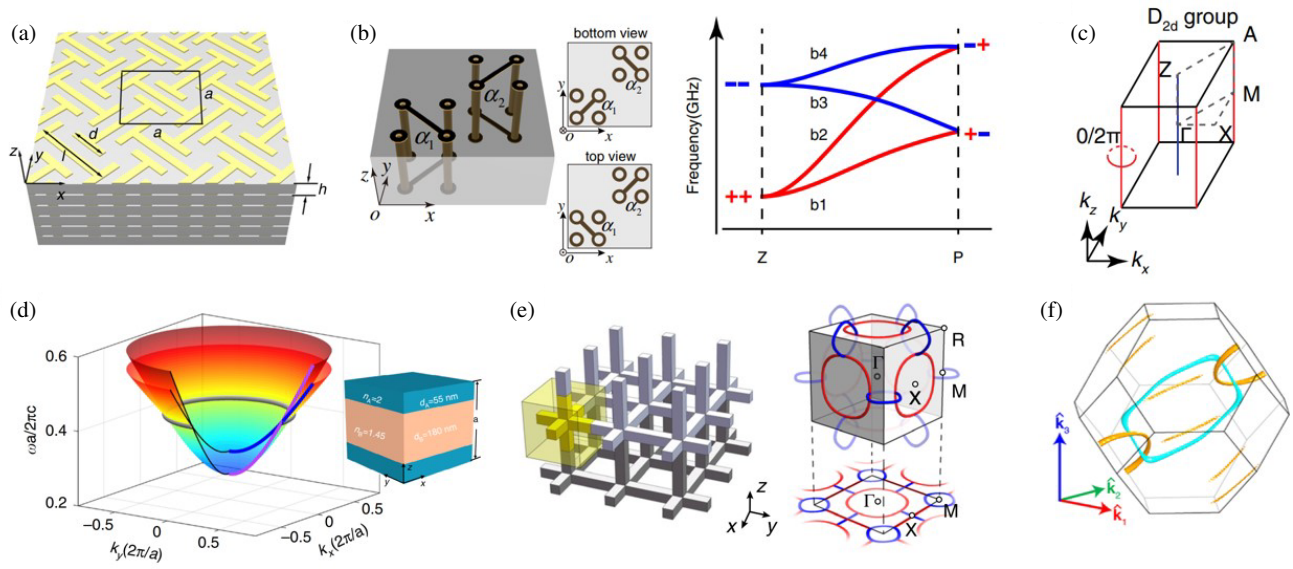

FIGURE 6. 3D photonic crystals possessing nodal lines. (a) Experimental observation of photonic nodal rings. (b) Observation of hourglass nodal lines. (c) Straight photonic nodal lines possessing quadrupole Berry curvature distribution. (d) Nodal rings of 1D photonic crystals in the visible region. (e) Nodal chains in 3D metallic-mesh photonic crystals. (f) Nodal links in dielectric photonic crystals.
Figures reproduced from: (a) Ref. [75], Copyright 2018, Springer Nature; (b) Ref. [76], Copyright 2019, American Physical Society; (c) Ref. [79], Copyright 2022, American Physical Society; (d) Ref. [80], Copyright 2022, Springer Nature; (e) Ref. [82], Copyright 2018, Springer Nature; (f) Ref. [83], Copyright 2021, American Chemical Society.

($k_x = k_y = \pi$), while two pairs of ideal Weyl points are located at the $k_z = 0$ plane.

Due to the complex symmetry requirements for stabilizing Dirac points, experimental observation of Dirac points in photonic crystals is particularly difficult. Utilizing electromagnetic dual symmetry, the first experimental demonstration of a Dirac semimetal in a classical system was achieved in a carefully designed metamaterial (Fig. 5(e)) [74]. Since Dirac points can be viewed as a combination of two Weyl points with opposite chirality, the Fermi arcs in Dirac semimetals are spin-polarized. In this metamaterial system, the spin-dependent surface states were also observed under circularly polarized light excitation.

3.3. Nodal Line

When two bands intersect, they can form not only point degeneracies in momentum space, but also line degeneracies, known as nodal lines. Nodal lines are typically classified by their shapes and how they connect with other nodal lines, such as rings, links and chains [87]. A nodal ring exhibits topological features, such as a π Berry phase threading through the ring [88, 89]. Due to this π Berry phase, topological surface states, known as the drumhead surface states, can be supported inside or outside the nodal ring. A nodal ring is not topologically charged and can be gapped or split into two Weyl points by introducing perturbations.

The first realization of a photonic nodal line semimetal occurred in a 3D double-gyroid photonic crystal [49]. However, due to the complex structure of double-gyroid photonic crystals, experimental observation of this nodal line structure has not yet been achieved. Instead, the first experimental observation of photonic nodal line degeneracies was accomplished in a metacrystal possessing glide and mirror symmetries (Fig. 6(a)) [75]. Early realizations of nodal line semimetals mostly relied on accidental degeneracies, making these nodal lines fragile and susceptible to perturbations even without symmetry breaking. It was found that by involving four bands instead of two, forming an hourglass-shaped band dispersion, a robust nodal line degeneracy resistant to symmetry-preserving perturbations can be realized. The photonic realization of such an hourglass nodal line was demonstrated in a metacrystal with three glide symmetries and D_{4h} point group symmetry (Fig. 6(b)) [76]. In addition to the ring-shaped nodal lines, a novel type of straight nodal lines was demonstrated, located at the hinges and central axis of the BZ (Fig. 6(c)). Protected by rotoinversion and T symmetries, these straight nodal lines exhibit quadratic band dispersion and give rise to a quadrupolar distribution of Berry curvature [79]. Instead of 3D photonic crystals, nodal line degeneracies were recently found in a 1D layer-stacked photonic crystal by considering off-axis momenta (Fig. 6(d)) [80]. Owing to its simple structure, the nodal ring and accompanying drumhead surface states were experimentally observed in the visible spectrum. Furthermore, by breaking P, this nodal line was gapped, and the π Berry phase evolved into a toroidal-shaped Berry flux, resulting in photonic ridge states.

When two nodal rings come into contact, they form a nodal chain. While the Berry phase encircling a single nodal line is π, the Berry phase around the chain point is zero (since $\pi + \pi = 0$ modulo 2π) [90]. In a 3D metallic-mesh photonic crystal, such photonic nodal chain degeneracies have been demonstrated [82]. As shown in Fig. 6(e), the nodal rings in the BZ are all interconnected, forming a chain. When two nodal

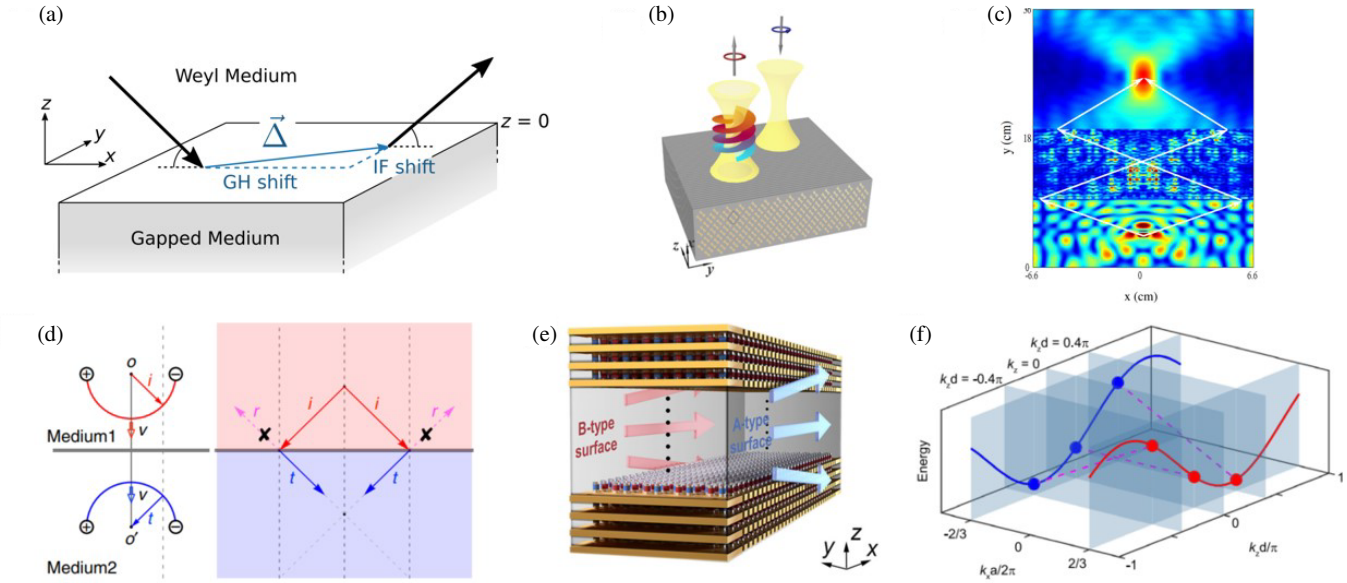

FIGURE 7. Topological effects in gapless 3D photonic crystals. (a) Reflected beam displacement on the interface of Weyl medium. (b) Vortical refection around Weyl points. (c) Veselago lens based on Weyl semimetals. (d) All-angle reflectionless negative refraction based on semicircle Fermi arcs. (e) Antichiral surface states in 3D magnetic Weyl photonic crystals. (f) Antichiral surface states in time-reversal-invariant photonic cyrstals.
Figures reproduced from: (a) Ref. [92], Copyright 2019, American Physical Society; (b) Ref. [93], Copyright 2020, American Physical Society; (c) Ref. [94], Copyright 2021, The Optica Society; (d) Ref. [95], Copyright 2022, Springer Nature; (e) Ref. [97], Copyright 2023, Springer Nature; (f) Ref. [98], Copyright 2023, Springer Nature.

rings approach even closer, they can merge to form a nodal link structure [91]. Since nodal links often involve multiple bands, recent studies in non-Abelian band topology have revealed that the topological charges of these nodal links can be described using quaternions. In a dielectric photonic crystal with a double-diamond structure, a nodal link carrying non-Abelian charges was demonstrated (Fig. 6(f)) [83].

3.4. Topological Effects Related to Gapless Phases

Based on the novel features of topological semimetals, various intriguing topological effects and light transport phenomena related to topological gapless phases have been extensively studied. For example, when beams in a Weyl medium reflect off an interface with a gapped medium, it has been found that the reflected beams experience a displacement analogous to the Goos-Hänchen or Imbert-Fedorov shifts, forming a half-vortex in the 2D surface momentum space (Fig. 7(a)) [92]. This effect is tied to both bulk geometrical properties and Fermi arc surface states, bridging the gap between topological surface states and bulk properties that have traditionally been studied separately. In addition, when a beam with spin angular momentum is incident onto a Weyl semimetal, the reflected beam is converted to the opposite spin angular momentum and acquires additional orbital angular momentum (Fig. 7(b)) [93]. Based on this vortical reflection around the Weyl points, spiraling Fermi arcs have been observed in a guided system where an air layer is sandwiched between a metallic plate and a Weyl semimetal.

It has been discovered that negative refraction can occur at the interface between a suitably designed Weyl medium and a normal dielectric medium when operating below the Weyl frequency. Utilizing this negative refraction property, a Veselago lens was demonstrated in a Weyl semimetal (Fig. 7(c)) [94]. In addition, it was found that by interfacing the Weyl medium with a perfect electric conductor (perfect magnetic conductor), the Fermi arc can form a semicircle, exhibiting a positive (negative) refractive index, which leads to the realization of reflectionless negative refraction (Fig. 7(d)) [95].

While chiral edge state is a hallmark of 2D Chern insulators, the antichiral edge state was recently proposed in a 2D modified Haldane model [96]. In contrast to chiral edge states that propagate in opposite directions along two parallel strip edges, the antichiral edge states exhibit co-propagation along two parallel strip edges. Recently, the antichiral transmission has been extended to 3D systems. The 3D modified Haldane model was constructed by stacking the 2D version along the z-axis. This 3D model was realized in a magnetic photonic crystal with precise on-site magnetization modulation (Fig. 7(e)) [97]. Instead of using gyromagnetic materials to break T, antichiral surface transport was also achieved in a T-invariant photonic crystal by constructing a gauge magnetic field (Fig. 7(f)) [98].

4. OTHER PROGRESS IN 3D TOPOLOGICAL PHOTONIC CRYSTALS

4.1. 3D Topological Phases in Photonic Crystals with Synthetic Dimensions

Beyond spatial dimensions, non-spatial DOFs, referred to as synthetic dimensions, have recently been found to offer new possibilities for realizing topological phases. By combining spatial dimensions with synthetic dimensions, we can construct

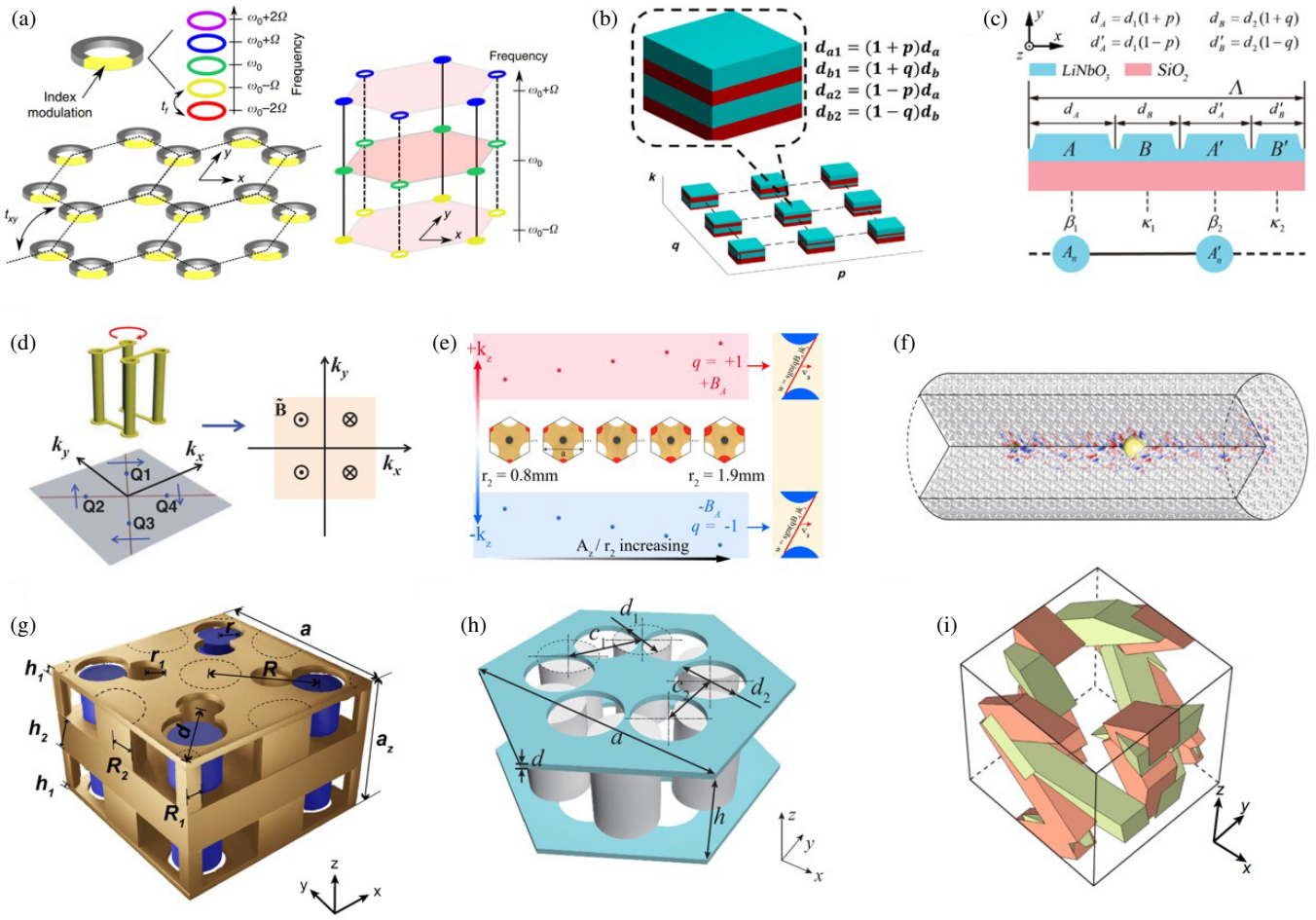

FIGURE 8. Other progress in 3D topological photonic crystals. (a) Realization of Weyl points in the 2D array of ring resonators. (b) Synthetic Weyl points in 1D photonic crystals. (c) Probing rotated Weyl physics in on-chip waveguide arrays. (d) Realization of chiral zero modes by designing artificial magnetic field. (e) Realization of co-propagating chiral zero modes. (f) One-way fiber modes in 3D photonic crystals with helical modulation. (g) Higher-order topological insulator phase in 3D metallic-cage photonic crystals. (h) Higher-order Dirac semimetal phase in photonic crystals. (i) Real higher-order Weyl semimetal phase in photonic crystals.
Figures reproduced from: (a) Ref. [100], Copyright 2016, Springer Nature; (b) Ref. [101], Copyright 2017, American Physical Society; (c) Ref. [102], Copyright 2021, American Physical Society; (d) Ref. [103], Copyright 2019, The American Association for the Advancement of Science; (e) Ref. [104], arXiv; (f) Ref. [105], Copyright 2018, Springer Nature; (g) Ref. [107], Research Square; (h) Ref. [108], Copyright 2022, American Physical Society; (i) Ref. [109], Copyright 2023, Springer Nature.

a higher-dimensional "synthetic space" [99]. In photonics, synthetic space can be created in two main ways. One approach is to treat a synthetic dimension as an additional spatial dimension, forming a lattice. For example, by considering the frequency dimension as a synthetic spatial dimension, a synthetic 3D lattice can be created by dynamically modulating a 2D array of ring resonators (Fig. 8(a)) [100]. With precise modulation, the coupling between modes in the frequency dimension can be finely controlled, enabling the realization of Weyl physics in this 2D resonator array.

Instead of forming a lattice, a synthetic parameter space can be created by exploiting the system's parameter dependencies, with the synthetic dimension functioning similarly to Bloch momentum. For example, replacing two Bloch momenta with two independent geometric parameters enables the realization of Weyl physics in a 3D synthetic space composed of two geometric parameters and one Bloch momentum. Using this concept, Weyl points were observed in 1D photonic crystals (Fig. 8(b)), where the vortical reflection phases confirmed the presence of synthetic Weyl points [101]. This idea was further demonstrated in a 1D waveguide array system on lithium niobate-on-insulator chips (Fig. 8(c)) [102]. The flexibility of synthetic space allows the orientation between two Weyl structures to be freely rotated, which is ideal for exploring Fermi arc reconstruction but difficult to achieve in conventional 3D Weyl semimetals due to lattice mismatch.

4.2. 3D Topological Photonic Crystals with Lattice Deformation

Intriguing topological phenomena can also emerge in systems with lattice deformation. One significant effect of lattice deformation is the introduction of a gauge field in Weyl systems. For instance, by rotating the saddle-shaped metallic coil in the unit cell, four Weyl points in the BZ rotate around the k_z-axis [103].

Through careful manipulation of different rotation angles for each individual unit cell at different locations, the entire system can be treated as a Weyl system under an external magnetic field (Fig. 8(d)). In this inhomogeneous 3D photonic crystal, chiral zero modes with unidirectional propagation were observed. Moreover, making the Weyl points with opposite chirality experience artificial magnetic fields in opposite directions, co-propagating chiral zero modes were demonstrated in a 3D magnetic photonic crystal (Fig. 8(e)) [104].

By introducing helical modulation into 3D lattices, a line defect can be created, accompanied by defect modes. In this case, the line defect acts as a "fiber core" within the 3D system, supporting 1D propagating modes [105]. By applying periodic modulation, one-way fiber modes were achieved in a 3D Weyl magnetic photonic crystal (Fig. 8(f)). These one-way defect modes reside within the band gap, and the number of modes is determined by the helix frequency.

4.3. Higher-Order Topological Phases in 3D Photonic Crystals

Recently, the discovery of higher-order topological phases has attracted significant attention due to its violation of the conventional bulk-boundary correspondence [106]. For instance, a 3D third-order topological insulator can host not only 2D surface states but also 1D hinge states and 0D corner states. These higher-order topological insulators (HOTIs) offer more DOFs for light manipulation. In 3D systems, there are two types of higher-order topological phases: octupole HOTIs, which possess quantized multipole moments, and Wannier-type HOTIs, which do not. While the realization of octupole HOTIs requires negative coupling — challenging to achieve in photonic crystals — the realization of Wannier-type HOTIs, which mimic a 3D Su-Schrieffer-Heeger (SSH) model, appears more feasible. However, due to the vectorial nature of the electromagnetic field, achieving a non-trivial complete band gap in 3D SSH-like photonic crystals is still difficult. In very recent, the experimental realization of the 3D SSH model was demonstrated in 3D tight-binding-like metal-cage photonic crystals (Fig. 8(g)) [107]. This photonic crystal mimics a tight-binding system with nearest-neighbor coupling, successfully simulating the 3D SSH model and observing the associated higher-order topological features.

Beyond topological insulators, higher-order topology has also been introduced into topological semimetals, where the surface states and lower-dimensional hinge states are allowed to coexist. For example, a higher-order Dirac semimetal was demonstrated in a layer-coupled deformed photonic honeycomb lattice (Fig. 8(h)) [108]. In this system, the 3D BZ is divided into two regions: a normal insulator phase and a HOTI phase. In the projected BZ, the Dirac points are connected by higher-order hinge states. In addition to higher-order Dirac semimetals, a higher-order Weyl semimetal was realized in a 3D metallic photonic crystal (Fig. 8(i)) [109]. In this system, the 3D BZ is divided by Weyl points into a Chern insulator phase and a generalized real Chern insulator phase. Protected by both the nonzero Chern number and the nontrivial generalized real Chern number, this system supports the coexistence of Fermi arc surface states and higher-order hinge states.

5. CONCLUSION AND OUTLOOK

Historically, 3D geometries have introduced richer and more complex physics into photonic research; the realization of 3D complete bandgap marks the advent of photonic crystals as a distinct field in modern photonics. Following a quite similar trajectory, the development of 3D topological photonic crystals is still in its infancy.

In recent years, significant breakthroughs, such as the realization of photonic topological insulators and topological semimetals, have demonstrated the 3D photonic crystal a promising platform for exploring novel physics. Further, new physics can still be found at these systems. For instance, axion insulators — 3D magnetic topological insulators that support chiral hinge states — have been proposed as a means of detecting dark-matter axionic particles in high-energy physics [110–115]. It has recently been found that axion insulator can have its photonic counterpart in 3D gyrotropic photonic crystals [116]. Moreover, the outer surfaces of the photonic axion insulator behave as fractional Chern insulators with a half-quantized Chern number. Such interaction between fractional and integer Chern numbers presents new avenues in topological physics.

While initial studies of 3D topological photonic crystals focused on mimicking condensed matter phenomena, future research may prioritize the applications of 3D topological phases. For instance, the low-loss light transport facilitated by topological edge modes has positioned photonic topological systems as promising platforms for optical communication [117–120]. Despite the current applications of topological light transmission are mainly concentrated on 2D systems, it is potential to develop topological 3D photonic circuits due to the diverse boundary manifestations in 3D topological photonic crystals, ranging from 0D localized modes to 2D propagating modes. The 3D topological photonic circuits are potential to enable robust and flexible light transport in 3D space.

In addition, microwave control plays a fundamental role in modern quantum computing algorithms, in which microwave resonators can mediate interactions between distant qubits and microwave pulses can be used for rotating qubits or generating entanglement [121, 122]. However, qubits are highly sensitive, and easy to decoherence due to the defects or fabrication imperfections [123–125]. Therefore, the implementation of microwave 3D topological photonic circuits, which provide robust and flexible light transport in 3D space, could offer a promising solution to mitigate these challenges in quantum computing.

Furthermore, recent studies have investigated the interaction between topological light and matter, leading to phenomena such as the emergence of helical topological polaritons [115, 116] and room-temperature valley polariton condensation [117, 118]. Distinct from the 2D counterparts, the omnidirectional bang gaps of 3D topological photonic crystals offer robust light confinement in all three spatial directions, enabling enhanced light-matter interactions. Thus, by leveraging corner or hinge states in 3D topological photonic crystals, it is potential to realize the topological cavities with ultra-high quality factors, which could find applications in fields such as

sensing [126, 127], Bose-Einstein condensation [128, 129] and polariton lasing [130, 131].

At the end of this review, it should be reminded that there are still some challenges to be addressed for reaching these exciting prospects. For example, implementing 3D topological photonic crystals for communication or lasing applications requires the realization of 3D topological phases in the communication and visible wavelength ranges. While certain 3D topological phases have been demonstrated in the infrared regime [65, 69, 132], the bulky nature of 3D photonic crystals still imposes considerable demands on advanced micro-nano fabrication techniques. Moreover, many realizations of 3D topological phases rely on metallic or gyromagnetic materials [44, 46, 47, 50, 97], which suffer from losses or weak magneto-optical responses in the optical domain, making the selection of suitable materials a critical challenge.

On a more optimistic note, even if extending 3D topological photonic crystals to the visible regime proves challenging, the intersection between microwave 3D topological photonic crystals and quantum computing can be a promising and exciting direction for future exploration.

ACKNOWLEDGEMENT

This work is supported by Singapore National Research Fundation Competitive Research Program under Grant No. NRF-CRP23-2019-0007, Singapore Ministry of Education Academic Research Fund Tier 2 under Grant No. MOE-T2EP50123-0007, and Tier 1 Grant No. RG139/22 and RG81/23.

REFERENCES

[1] Yablonovitch, E., "Inhibited spontaneous emission in solid-state physics and electronics," *Physical Review Letters*, Vol. 58, No. 20, 2059, 1987.

[2] John, S., "Strong localization of photons in certain disordered dielectric superlattices," *Physical Review Letters*, Vol. 58, No. 23, 2486, 1987.

[3] Ho, K. M., C. T. Chan, and C. M. Soukoulis, "Existence of a photonic gap in periodic dielectric structures," *Physical Review Letters*, Vol. 65, No. 25, 3152, 1990.

[4] Sözüer, H. S., J. W. Haus, and R. Inguva, "Photonic bands: Convergence problems with the plane-wave method," *Physical Review B*, Vol. 45, No. 24, 13962, 1992.

[5] Sözüer, H. S. and J. P. Dowling, "Photonic band calculations for woodpile structures," *Journal of Modern Optics*, Vol. 41, No. 2, 231–239, 1994.

[6] Busch, K. and S. John, "Photonic band gap formation in certain self-organizing systems," *Physical Review E*, Vol. 58, No. 3, 3896, 1998.

[7] Lin, S.-y., J. G. Fleming, D. L. Hetherington, B. K. Smith, R. Biswas, K. M. Ho, M. M. Sigalas, W. Zubrzycki, S. R. Kurtz, and J. Bur, "A three-dimensional photonic crystal operating at infrared wavelengths," *Nature*, Vol. 394, No. 6690, 251–253, 1998.

[8] Vlasov, Y. A., X.-Z. Bo, J. C. Sturm, and D. J. Norris, "On-chip natural assembly of silicon photonic bandgap crystals," *Nature*, Vol. 414, No. 6861, 289–293, 2001.

[9] Ishizaki, K., K. Suzuki, and S. Noda, "Fabrication of 3D photonic crystals toward arbitrary manipulation of photons in three dimensions," in *Photonics*, Vol. 3, No. 2, 36, 2016.

[10] Ogawa, S., M. Imada, S. Yoshimoto, M. Okano, and S. Noda, "Control of light emission by 3D photonic crystals," *Science*, Vol. 305, No. 5681, 227–229, 2004.

[11] Qi, M., E. Lidorikis, P. T. Rakich, S. G. Johnson, J. D. Joannopoulos, E. P. Ippen, and H. I. Smith, "A three-dimensional optical photonic crystal with designed point defects," *Nature*, Vol. 429, No. 6991, 538–542, 2004.

[12] Imada, M., L. H. Lee, M. Okano, S. Kawashima, and S. Noda, "Development of three-dimensional photonic-crystal waveguides at optical-communication wavelengths," *Applied Physics Letters*, Vol. 88, No. 17, 171107, 2006.

[13] Rinne, S. A., F. García-Santamaría, and P. V. Braun, "Embedded cavities and waveguides in three-dimensional silicon photonic crystals," *Nature Photonics*, Vol. 2, No. 1, 52–56, 2008.

[14] Ishizaki, K., M. Koumura, K. Suzuki, K. Gondaira, and S. Noda, "Realization of three-dimensional guiding of photons in photonic crystals," *Nature Photonics*, Vol. 7, No. 2, 133–137, 2013.

[15] Ozawa, T., H. M. Price, A. Amo, N. Goldman, M. Hafezi, L. Lu, M. C. Rechtsman, D. Schuster, J. Simon, O. Zilberberg, and I. Carusotto, "Topological photonics," *Reviews of Modern Physics*, Vol. 91, No. 1, 015006, 2019.

[16] Kim, M., Z. Jacob, and J. Rho, "Recent advances in 2D, 3D and higher-order topological photonics," *Light: Science & Applications*, Vol. 9, No. 1, 130, 2020.

[17] Price, H., Y. Chong, A. Khanikaev, H. Schomerus, L. J. Maczewsky, M. Kremer, M. Heinrich, A. Szameit, O. Zilberberg, Y. Yang, and e. al., "Roadmap on topological photonics," *Journal of Physics: Photonics*, Vol. 4, No. 3, 032501, 2022.

[18] Tang, G.-J., X.-T. He, F.-L. Shi, J.-W. Liu, X.-D. Chen, and J.-W. Dong, "Topological photonic crystals: Physics, designs, and applications," *Laser & Photonics Reviews*, Vol. 16, No. 4, 2100300, 2022.

[19] Khanikaev, A. B. and G. Shvets, "Two-dimensional topological photonics," *Nature Photonics*, Vol. 11, No. 12, 763–773, 2017.

[20] Wang, Z., Y. D. Chong, J. D. Joannopoulos, and M. Soljačić, "Reflection-free one-way edge modes in a gyromagnetic photonic crystal," *Physical Review Letters*, Vol. 100, No. 1, 013905, 2008.

[21] Wang, Z., Y. Chong, J. D. Joannopoulos, and M. Soljačić, "Observation of unidirectional backscattering-immune topological electromagnetic states," *Nature*, Vol. 461, No. 7265, 772–775, 2009.

[22] Ao, X., Z. Lin, and C. T. Chan, "One-way edge mode in a magneto-optical honeycomb photonic crystal," *Physical Review B*, Vol. 80, No. 3, 033105, 2009.

[23] Fu, J.-X., R.-J. Liu, and Z.-Y. Li, "Robust one-way modes in gyromagnetic photonic crystal waveguides with different interfaces," *Applied Physics Letters*, Vol. 97, No. 4, 041112, 2010.

[24] Chen, W.-J., S.-J. Jiang, X.-D. Chen, B. Zhu, L. Zhou, J.-W. Dong, and C. T. Chan, "Experimental realization of photonic topological insulator in a uniaxial metacrystal waveguide," *Nature Communications*, Vol. 5, No. 1, 5782, 2014.

[25] Ma, T., A. B. Khanikaev, S. H. Mousavi, and G. Shvets, "Guiding electromagnetic waves around sharp corners: Topologically protected photonic transport in metawaveguides," *Physical Review Letters*, Vol. 114, No. 12, 127401, 2015.

[26] Wu, L.-H. and X. Hu, "Scheme for achieving a topological photonic crystal by using dielectric material," *Physical Review Letters*, Vol. 114, No. 22, 223901, 2015.

[27] Barik, S., A. Karasahin, C. Flower, T. Cai, H. Miyake, W. DeGottardi, M. Hafezi, and E. Waks, "A topological quantum optics interface," *Science*, Vol. 359, No. 6376, 666–668, 2018.

[28] Ma, T. and G. Shvets, "All-Si valley-hall photonic topological insulator," *New Journal of Physics*, Vol. 18, No. 2, 025012, 2016.

[29] Chen, X.-D., F.-L. Zhao, M. Chen, and J.-W. Dong, "Valley-contrasting physics in all-dielectric photonic crystals: Orbital angular momentum and topological propagation," *Physical Review B*, Vol. 96, No. 2, 020202(R), 2017.

[30] Gao, F., H. Xue, Z. Yang, K. Lai, Y. Yu, X. Lin, Y. Chong, G. Shvets, and B. Zhang, "Topologically protected refraction of robust kink states in valley photonic crystals," *Nature Physics*, Vol. 14, No. 2, 140–144, 2018.

[31] He, X.-T., E.-T. Liang, J.-J. Yuan, H.-Y. Qiu, X.-D. Chen, F.-L. Zhao, and J.-W. Dong, "A silicon-on-insulator slab for topological valley transport," *Nature Communications*, Vol. 10, No. 1, 872, 2019.

[32] Chen, X.-D., Z.-X. Gao, X. Cui, H.-C. Mo, W.-J. Chen, R.-Y. Zhang, C. T. Chan, and J.-W. Dong, "Realization of time-reversal invariant photonic topological anderson insulators," *Physical Review Letters*, Vol. 133, No. 13, 133802, 2024.

[33] Ma, J., X. Xi, and X. Sun, "Topological photonic integrated circuits based on valley kink states," *Laser & Photonics Reviews*, Vol. 13, No. 12, 1900087, 2019.

[34] Yang, Y., Y. Yamagami, X. Yu, P. Pitchappa, J. Webber, B. Zhang, M. Fujita, T. Nagatsuma, and R. Singh, "Terahertz topological photonics for on-chip communication," *Nature Photonics*, Vol. 14, No. 7, 446–451, 2020.

[35] Wang, W., Y. J. Tan, T. C. Tan, A. Kumar, P. Pitchappa, P. Szriftgiser, G. Ducournau, and R. Singh, "On-chip topological beamformer for multi-link terahertz 6G to XG wireless," *Nature*, Vol. 632, No. 8025, 522–527, 2024.

[36] Bahari, B., A. Ndao, F. Vallini, A. E. Amili, Y. Fainman, and B. Kanté, "Nonreciprocal lasing in topological cavities of arbitrary geometries," *Science*, Vol. 358, No. 6363, 636–640, 2017.

[37] Bandres, M. A., S. Wittek, G. Harari, M. Parto, J. Ren, M. Segev, D. N. Christodoulides, and M. Khajavikhan, "Topological insulator laser: Experiments," *Science*, Vol. 359, No. 6381, 2018.

[38] Zeng, Y., U. Chattopadhyay, B. Zhu, B. Qiang, J. Li, Y. Jin, L. Li, A. G. Davies, E. H. Linfield, B. Zhang, Y. Chong, and Q. J. Wang, "Electrically pumped topological laser with valley edge modes," *Nature*, Vol. 578, No. 7794, 246–250, 2020.

[39] Yu, N. and F. Capasso, "Flat optics with designer metasurfaces," *Nature Materials*, Vol. 13, No. 2, 139–150, 2014.

[40] Liu, W. and H. C. T. Chen, "Diffractive metalens: From fundamentals, practical applications to current trends," *Advances in Physics: X*, Vol. 5, No. 1, 1742584, 2020.

[41] Hasan, M. Z. and C. L. Kane, "Colloquium: Topological insulators," *Reviews of Modern Physics*, Vol. 82, No. 4, 3045–3067, 2010.

[42] Qi, X.-L. and S.-C. Zhang, "Topological insulators and superconductors," *Reviews of Modern Physics*, Vol. 83, No. 4, 1057–1110, 2011.

[43] Armitage, N. P., E. J. Mele, and A. Vishwanath, "Weyl and Dirac semimetals in three-dimensional solids," *Reviews of Modern Physics*, Vol. 90, No. 1, 015001, 2018.

[44] Liu, G.-G., Z. Gao, Q. Wang, X. Xi, Y.-H. Hu, M. Wang, C. Liu, X. Lin, L. Deng, S. A. Yang, *et al.*, "Topological Chern vectors in three-dimensional photonic crystals," *Nature*, Vol. 609, No. 7929, 925–930, 2022.

[45] Slobozhanyuk, A., S. H. Mousavi, X. Ni, D. Smirnova, Y. S. Kivshar, and A. B. Khanikaev, "Three-dimensional all-dielectric photonic topological insulator," *Nature Photonics*, Vol. 11, 130–136, 2017.

[46] Yang, Y., Z. Gao, H. Xue, L. Zhang, M. He, Z. Yang, R. Singh, Y. Chong, B. Zhang, and H. Chen, "Realization of a three-dimensional photonic topological insulator," *Nature*, Vol. 565, No. 7741, 622–626, 2019.

[47] Yang, B., Q. Guo, B. Tremain, R. Liu, L. E. Barr, Q. Yan, W. Gao, H. Liu, Y. Xiang, J. Chen, *et al.*, "Ideal weyl points and helicoid surface states in artificial photonic crystal structures," *Science*, Vol. 359, No. 6379, 1013–1016, 2018.

[48] Chen, W.-J., M. Xiao, and C. T. Chan, "Photonic crystals possessing multiple weyl points and the experimental observation of robust surface states," *Nature Communications*, Vol. 7, No. 1, 13038, 2016.

[49] Lu, L., L. Fu, J. D. Joannopoulos, and M. Soljačić, "Weyl points and line nodes in gyroid photonic crystals," *Nature Photonics*, Vol. 7, No. 4, 294–299, 2013.

[50] Devescovi, C., M. García-Díez, I. Robredo, M. B. d. Paz, J. Lasa-Alonso, B. Bradlyn, J. L. Mañes, M. G. Vergniory, and A. García-Etxarri, "Cubic 3D Chern photonic insulators with orientable large Chern vectors," *Nature Communications*, Vol. 12, No. 1, 7330, 2021.

[51] Devescovi, C., M. García-Díez, B. Bradlyn, J. L. Mañes, M. G. Vergniory, and A. García-Etxarri, "Vectorial bulk-boundary correspondence for 3D photonic Chern insulators," *Advanced Optical Materials*, Vol. 10, No. 20, 2200475, 2022.

[52] Lu, L., C. Fang, L. Fu, S. G. Johnson, J. D. Joannopoulos, and M. Soljačić, "Symmetry-protected topological photonic crystal in three dimensions," *Nature Physics*, Vol. 12, No. 4, 337–340, 2016.

[53] Ochiai, T., "Gapless surface states originating from accidentally degenerate quadratic band touching in a three-dimensional tetragonal photonic crystal," *Physical Review A*, Vol. 96, No. 4, 043842, 2017.

[54] Kim, M., Z. Wang, Y. Yang, H. T. Teo, J. Rho, and B. Zhang, "Three-dimensional photonic topological insulator without spin-orbit coupling," *Nature Communications*, Vol. 13, No. 1, 3499, 2022.

[55] Lustig, E., L. J. Maczewsky, J. Beck, T. Biesenthal, M. Heinrich, Z. Yang, Y. Plotnik, A. Szameit, and M. Segev, "Photonic topological insulator induced by a dislocation in three dimensions," *Nature*, Vol. 609, No. 7929, 931–935, 2022.

[56] Haldane, F. D. M., "Model for a quantum Hall effect without landau levels: Condensed-matter realization of the "parity anomaly"," *Physical Review Letters*, Vol. 61, No. 18, 2015, 1988.

[57] Halperin, B. I., "Possible states for a three-dimensional electron gas in a strong magnetic field," *Japanese Journal of Applied Physics*, Vol. 26, No. S3-3, 1913, 1987.

[58] Kohmoto, M., B. I. Halperin, and Y.-S. Wu, "Diophantine equation for the three-dimensional quantum Hall effect," *Physical Review B*, Vol. 45, No. 23, 13488, 1992.

[59] Fu, L., C. L. Kane, and E. J. Mele, "Topological insulators in three dimensions," *Physical Review Letters*, Vol. 98, No. 10, 106803, 2007.

[60] Bravo-Abad, J., L. Lu, L. Fu, H. Buljan, and M. Soljačić, "Weyl points in photonic-crystal superlattices," *2D Materials*, Vol. 2, No. 3, 034013, 2015.

[61] Lu, L., Z. Wang, D. Ye, L. Ran, L. Fu, J. D. Joannopoulos, and M. Soljačić, "Experimental observation of Weyl points," *Science*, Vol. 349, No. 6248, 622–624, 2015.

[62] Wang, L., S.-K. Jian, and H. Yao, "Topological photonic crystal with equifrequency Weyl points," *Physical Review A*, Vol. 93, No. 6, 061801, 2016.

[63] Chang, M.-L., M. Xiao, W.-J. Chen, and C. T. Chan, "Multiple Weyl points and the sign change of their topological charges in woodpile photonic crystals," *Physical Review B*, Vol. 95, No. 12, 125136, 2017.

[64] Yang, B., Q. Guo, B. Tremain, L. E. Barr, W. Gao, H. Liu, B. Béri, Y. Xiang, D. Fan, A. P. Hibbins, and S. Zhang, "Direct observation of topological surface-state arcs in photonic metamaterials," *Nature Communications*, Vol. 8, No. 1, 97, 2017.

[65] Vaidya, S., J. Noh, A. Cerjan, C. Jörg, G. V. Freymann, and M. C. Rechtsman, "Observation of a charge-2 photonic Weyl point in the infrared," *Physical Review Letters*, Vol. 125, No. 25, 253902, 2020.

[66] Yang, Y., Z. Gao, X. Feng, Y.-X. Huang, P. Zhou, S. A. Yang, Y. Chong, and B. Zhang, "Ideal unconventional Weyl point in a chiral photonic metamaterial," *Physical Review Letters*, Vol. 125, No. 14, 143001, 2020.

[67] Takahashi, S., S. Tamaki, K. Yamashita, T. Yamaguchi, T. Ueda, and S. Iwamoto, "Transmission properties of microwaves at an optical Weyl point in a three-dimensional chiral photonic crystal," *Optics Express*, Vol. 29, No. 17, 27 127–27 136, 2021.

[68] Chen, Q., F. Chen, Y. Pan, C. Cui, Q. Yan, L. Zhang, Z. Gao, S. A. Yang, Z.-M. Yu, H. Chen, B. Zhang, and B. Zhang, "Discovery of a maximally charged Weyl point," *Nature Communications*, Vol. 13, No. 1, 7359, 2022.

[69] Jörg, C., S. Vaidya, J. Noh, A. Cerjan, S. Augustine, G. v. Freymann, and M. C. Rechtsman, "Observation of quadratic (charge-2) weyl point splitting in near-infrared photonic crystals," *Laser & Photonics Reviews*, Vol. 16, No. 1, 2100452, 2022.

[70] Goi, E., Z. Yue, B. P. Cumming, and M. Gu, "Observation of type I photonic Weyl points in optical frequencies," *Laser & Photonics Reviews*, Vol. 12, No. 2, 1700271, 2018.

[71] Wang, H., L. Xu, H. Chen, and J.-H. Jiang, "Three-dimensional photonic Dirac points stabilized by point group symmetry," *Physical Review B*, Vol. 93, No. 23, 235155, 2016.

[72] Wang, H.-X., Y. Chen, Z. H. Hang, H.-Y. Kee, and J.-H. Jiang, "Type-ii dirac photons," *Npj Quantum Materials*, Vol. 2, No. 1, 54, 2017.

[73] Long, S., J. Yang, H. Wang, Z. Yu, B. Yang, Q. Guo, Y. Xiang, L. Xia, and S. Zhang, "Dirac-Weyl semimetal in photonic metacrystals," *Optics Letters*, Vol. 48, No. 9, 2349–2352, 2023.

[74] Guo, Q., O. You, B. Yang, J. B. Sellman, E. Blythe, H. Liu, Y. Xiang, J. Li, D. Fan, J. Chen, C. T. Chan, and S. Zhang, "Observation of three-dimensional photonic Dirac points and spin-polarized surface arcs," *Physical Review Letters*, Vol. 122, No. 20, 203903, 2019.

[75] Gao, W., B. Yang, B. Tremain, H. Liu, Q. Guo, L. Xia, A. P. Hibbins, and S. Zhang, "Experimental observation of photonic nodal line degeneracies in metacrystals," *Nature Communications*, Vol. 9, No. 1, 950, 2018.

[76] Xia, L., Q. Guo, B. Yang, J. Han, C.-X. Liu, W. Zhang, and S. Zhang, "Observation of hourglass nodal lines in photonics," *Physical Review Letters*, Vol. 122, No. 10, 103903, 2019.

[77] Xiong, Z., R.-Y. Zhang, R. Yu, C. T. Chan, and Y. Chen, "Hidden-symmetry-enforced nexus points of nodal lines in layer-stacked dielectric photonic crystals," *Light: Science & Applications*, Vol. 9, No. 1, 176, 2020.

[78] Yang, E., B. Yang, O. You, H.-C. Chan, P. Mao, Q. Guo, S. Ma, L. Xia, D. Fan, Y. Xiang, and S. Zhang, "Observation of non-Abelian nodal links in photonics," *Physical Review Letters*, Vol. 125, No. 3, 033901, 2020.

[79] Wang, D., B. Yang, R.-Y. Zhang, W.-J. Chen, Z. Q. Zhang, S. Zhang, and C. T. Chan, "Straight photonic nodal lines with quadrupole Berry curvature distribution and superimaging "fermi arcs"," *Physical Review Letters*, Vol. 129, No. 4, 043602, 2022.

[80] Deng, W.-M., Z.-M. Chen, M.-Y. Li, C.-H. Guo, Z.-T. Tian, K.-X. Sun, X.-D. Chen, W.-J. Chen, and J.-W. Dong, "Ideal nodal rings of one-dimensional photonic crystals in the visible region," *Light: Science & Applications*, Vol. 11, No. 1, 134, 2022.

[81] Yang, J., S. Long, H. Wang, Z. Yu, B. Yang, Q. Guo, Y. Xiang, L. Xia, and S. Zhang, "Coexistence of Dirac points and nodal chains in photonic metacrystal," *Optics Express*, Vol. 31, No. 11, 17 943–17 949, 2023.

[82] Yan, Q., R. Liu, Z. Yan, B. Liu, H. Chen, Z. Wang, and L. Lu, "Experimental discovery of nodal chains," *Nature Physics*, Vol. 14, No. 5, 461–464, 2018.

[83] Park, H., S. Wong, X. Zhang, and S. S. Oh, "Non-abelian charged nodal links in a dielectric photonic crystal," *ACS Photonics*, Vol. 8, No. 9, 2746–2754, 2021.

[84] Kim, M., D. Lee, D. Lee, and J. Rho, "Topologically nontrivial photonic nodal surface in a photonic metamaterial," *Physical Review B*, Vol. 99, No. 23, 235423, 2019.

[85] Wang, D., H. Jia, Q. Yang, J. Hu, Z. Q. Zhang, and C. T. Chan, "Intrinsic triple degeneracy point bounded by nodal surfaces in chiral photonic crystal," *Physical Review Letters*, Vol. 130, No. 20, 203802, 2023.

[86] Fang, C., L. Lu, J. Liu, and L. Fu, "Topological semimetals with helicoid surface states," *Nature Physics*, Vol. 12, No. 10, 936–941, 2016.

[87] Park, H., W. Gao, X. Zhang, and S. S. Oh, "Nodal lines in momentum space: Topological invariants and recent realizations in photonic and other systems," *Nanophotonics*, Vol. 11, No. 11, 2779–2801, 2022.

[88] Fang, C., Y. Chen, H.-Y. Kee, and L. Fu, "Topological nodal line semimetals with and without spin-orbital coupling," *Physical Review B*, Vol. 92, No. 8, 081201, 2015.

[89] Fang, C., H. Weng, X. Dai, and Z. Fang, "Topological nodal line semimetals," *Chinese Physics B*, Vol. 25, No. 11, 117106, 2016.

[90] Bzdušek, T., Q. Wu, A. Rüegg, M. Sigrist, and A. A. Soluyanov, "Nodal-chain metals," *Nature*, Vol. 538, No. 7623, 75–78, 2016.

[91] Yan, Z., R. Bi, H. Shen, L. Lu, S.-C. Zhang, and Z. Wang, "Nodal-link semimetals," *Physical Review B*, Vol. 96, No. 4, 041103, 2017.

[92] Chattopadhyay, U., L.-k. Shi, B. Zhang, J. C. W. Song, and Y. D. Chong, "Fermi-Arc-induced vortex structure in Weyl beam shifts," *Physical Review Letters*, Vol. 122, No. 6, 066602, 2019.

[93] Cheng, H., W. Gao, Y. Bi, W. Liu, Z. Li, Q. Guo, Y. Yang, O. You, J. Feng, *et al.*, "Vortical reflection and spiraling Fermi arcs with Weyl metamaterials," *Physical Review Letters*, Vol. 125, No. 9, 093904, 2020.

[94] Yang, Y., Y. Bi, L. Peng, B. Yang, S. Ma, H.-C. Chan, Y. Xiang, and S. Zhang, "Veselago lensing with weyl metamaterials," *Optica*, Vol. 8, No. 2, 249–254, 2021.

[95] Liu, Y., G. P. Wang, J. B. Pendry, and S. Zhang, "All-angle reflectionless negative refraction with ideal photonic Weyl metamaterials," *Light: Science & Applications*, Vol. 11, No. 1, 276, 2022.

[96] Colomes, E. and M. Franz, "Antichiral edge states in a modified haldane nanoribbon," *Physical Review Letters*, Vol. 120, 086603, 2018.

[97] Xi, X., B. Yan, L. Yang, Y. Meng, Z.-X. Zhu, J.-M. Chen, Z. Wang, P. Zhou, P. P. Shum, Y. Yang, *et al.*, "Topological antichiral surface states in a magnetic Weyl photonic crystal," *Nature Communications*, Vol. 14, No. 1, 1991, 2023.

[98] Liu, J.-W., F.-L. Shi, K. Shen, X.-D. Chen, K. Chen, W.-J. Chen, and J.-W. Dong, "Antichiral surface states in time-reversal-invariant photonic semimetals," *Nature Communications*, Vol. 14, No. 1, 2027, 2023.

[99] Yuan, L., Q. Lin, M. Xiao, and S. Fan, "Synthetic dimension in photonics," *Optica*, Vol. 5, No. 11, 1396–1405, 2018.

[100] Lin, Q., M. Xiao, L. Yuan, and S. Fan, "Photonic Weyl point in a two-dimensional resonator lattice with a synthetic frequency dimension," *Nature Communications*, Vol. 7, No. 1, 13731, 2016.

[101] Wang, Q., M. Xiao, H. Liu, S. Zhu, and C. T. Chan, "Optical interface states protected by synthetic Weyl points," *Physical Review X*, Vol. 7, No. 3, 031032, 2017.

[102] Yan, Z.-W., Q. Wang, M. Xiao, Y.-L. Zhao, S.-N. Zhu, and H. Liu, "Probing rotated Weyl physics on nonlinear lithium niobate-on-insulator chips," *Physical Review Letters*, Vol. 127, No. 1, 013901, 2021.

[103] Jia, H., R. Zhang, W. Gao, Q. Guo, B. Yang, J. Hu, Y. Bi, Y. Xiang, C. Liu, and S. Zhang, "Observation of chiral zero mode in inhomogeneous three-dimensional Weyl metamaterials," *Science*, Vol. 363, No. 6423, 148–151, 2019.

[104] Li, Z., S. Ma, S. Li, O. you, Y. Liu, Q. Yang, Y. Xiang, P. Zhou, and S. Zhang, "Observation of co-propagating chiral zero modes in magnetic photonic crystals," *ArXiv Preprint ArXiv:2407.03390*, 2024.

[105] Lu, L., H. Gao, and Z. Wang, "Topological one-way fiber of second Chern number," *Nature Communications*, Vol. 9, No. 1, 5384, 2018.

[106] Benalcazar, W. A., B. A. Bernevig, and T. L. Hughes, "Quantized electric multipole insulators," *Science*, Vol. 357, No. 6346, 61–66, 2017.

[107] Wang, Z., Y. Meng, B. Yan, D. Zhao, L. Yang, J.-M. Chen, M.-Q. Cheng, T. Xiao, P. P. Shum, G.-G. Liu, *et al.*, "Realization of a three-dimensional photonic higher-order topological insulator," *ArXiv Preprint ArXiv:2404.05649*, 2024.

[108] Wang, Z., D. Liu, H. T. Teo, Q. Wang, H. Xue, and B. Zhang, "Higher-order dirac semimetal in a photonic crystal," *Physical Review B*, Vol. 105, No. 6, L060101, 2022.

[109] Pan, Y., C. Cui, Q. Chen, F. Chen, L. Zhang, Y. Ren, N. Han, W. Li, X. Li, Z.-M. Yu, H. Chen, and Y. Yang, "Real higher-order Weyl photonic crystal," *Nature Communications*, Vol. 14, No. 1, 6636, 2023.

[110] Li, R., J. Wang, X.-L. Qi, and S.-C. Zhang, "Dynamical axion field in topological magnetic insulators," *Nature Physics*, Vol. 6, No. 4, 284–288, 2010.

[111] Millar, A. J., G. G. Raffelt, J. Redondo, and F. D. Steffen, "Dielectric haloscopes to search for axion dark matter: Theoretical foundations," *Journal of Cosmology and Astroparticle Physics*, Vol. 2017, No. 01, 061, 2017.

[112] Yokoi, N. and E. Saitoh, "Stimulated emission of dark matter axion from condensed matter excitations," *Journal of High Energy Physics*, Vol. 2018, No. 1, 1–21, 2018.

[113] Marsh, D. J. E., K. C. Fong, E. W. Lentz, L. Šmejkal, and M. N. Ali, "Proposal to detect dark matter using axionic topological antiferromagnets," *Physical Review Letters*, Vol. 123, No. 12, 121601, 2019.

[114] Lawson, M., A. J. Millar, M. Pancaldi, E. Vitagliano, and F. Wilczek, "Tunable axion plasma haloscopes," *Physical Review Letters*, Vol. 123, No. 14, 141802, 2019.

[115] Chigusa, S., T. Moroi, and K. Nakayama, "Axion/Hidden-photon dark matter conversion into condensed matter axion," *Journal of High Energy Physics*, Vol. 2021, No. 8, 1–33, 2021.

[116] Devescovi, C., A. Morales-Pérez, Y. Hwang, M. García-Díez, I. Robredo, J. L. Mañes, B. Bradlyn, A. García-Etxarri, and M. G. Vergniory, "Axion topology in photonic crystal domain walls," *Nature Communications*, Vol. 15, No. 1, 6814, 2024.

[117] Wu, Y., C. Li, X. Hu, Y. Ao, Y. Zhao, and Q. Gong, "Applications of topological photonics in integrated photonic devices," *Advanced Optical Materials*, Vol. 5, No. 18, 1700357, 2017.

[118] Blanco-Redondo, A., "Topological nanophotonics: Toward robust quantum circuits," *Proceedings of the IEEE*, Vol. 108, No. 5, 837–849, 2020.

[119] Ota, Y., K. Takata, T. Ozawa, A. Amo, Z. Jia, B. Kante, M. Notomi, Y. Arakawa, and S. Iwamoto, "Active topological photonics," *Nanophotonics*, Vol. 9, No. 3, 547–567, 2020.

[120] Iwamoto, S., Y. Ota, and Y. Arakawa, "Recent progress in topological waveguides and nanocavities in a semiconductor photonic crystal platform," *Optical Materials Express*, Vol. 11, No. 2, 319–337, 2021.

[121] Barzanjeh, S., S. Guha, C. Weedbrook, D. Vitali, J. H. Shapiro, and S. Pirandola, "Microwave quantum illumination," *Physical Review Letters*, Vol. 114, No. 8, 080503, 2015.

[122] Xiang, L., W. Jiang, Z. Bao, Z. Song, S. Xu, K. Wang, J. Chen, F. Jin, X. Zhu, Z. Zhu, and e. al., "Long-lived topological time-crystalline order on a quantum processor," *Nature Communications*, Vol. 15, No. 1, 8963, 2024.

[123] Schlosshauer, M., "Decoherence, the measurement problem, and interpretations of quantum mechanics," *Reviews of Modern physics*, Vol. 76, No. 4, 1267–1305, 2004.

[124] Albash, T. and D. A. Lidar, "Decoherence in adiabatic quantum computation," *Physical Review A*, Vol. 91, No. 6, 062320, 2015.

[125] Schlosshauer, M., "Quantum decoherence," *Physics Reports*, Vol. 831, 1–57, 2019.

[126] Cheng, Q., S. Wang, J. Lv, and N. Liu, "Topological photonic crystal biosensor with valley edge modes based on a silicon-on-insulator slab," *Optics Express*, Vol. 30, No. 7, 10 792–10 801, 2022.

[127] Deng, W., W. Zhu, T. Chen, H. Sun, and X. Zhang, "Ultra-sensitive integrated circuit sensors based on high-order non-Hermitian topological physics," *Science advances*, Vol. 10, No. 38, eadp6905, 2024.

[128] Deng, H., H. Haug, and Y. Yamamoto, "Exciton-polariton bose-einstein condensation," *Reviews of modern physics*, Vol. 82, No. 2, 1489–1537, 2010.

[129] Byrnes, T., N. Y. Kim, and Y. Yamamoto, "Exciton-polariton condensates," *Nature Physics*, Vol. 10, No. 11, 803–813, 2014.

[130] Fraser, M. D., S. Höfling, and Y. Yamamoto, "Physics and applications of exciton–polariton lasers," *Nature materials*, Vol. 15, No. 10, 1049–1052, 2016.

[131] Luo, S., H. Zhou, L. Zhang, and Z. Chen, "Nanophotonics of microcavity exciton-polaritons," *Applied Physics Reviews*, Vol. 10, No. 1, 011316, 2023.

[132] Peng, S., R. Zhang, V. H. Chen, E. T. Khabiboulline, P. Braun, and H. A. Atwater, "Three-dimensional single gyroid photonic crystals with a mid-infrared bandgap," *ACS Photonics*, Vol. 3, No. 6, 1131–1137, 2016.